Forschungszentrum Karlsruhe
in der Helmholtz-Gemeinschaft

Wissenschaftliche Berichte
FZKA 6968

Analysis of Hydrogen Production in QUENCH Bundle Tests

M. Steinbrück

Institut für Materialforschung
Programm Nukleare Sicherheitsforschung

Mai 2004

Forschungszentrum Karlsruhe

in der Helmholtz-Gemeinschaft

Wissenschaftliche Berichte

FZKA 6968

Analysis of Hydrogen Production in QUENCH Bundle Tests

M. Steinbrück

Institut für Materialforschung

Programm Nukleare Sicherheitsforschung

Forschungszentrum Karlsruhe GmbH, Karlsruhe

2004

Impressum der Print-Ausgabe:

Als Manuskript gedruckt
Für diesen Bericht behalten wir uns alle Rechte vor

Forschungszentrum Karlsruhe GmbH
Postfach 3640, 76021 Karlsruhe

Mitglied der Hermann von Helmholtz-Gemeinschaft
Deutscher Forschungszentren (HGF)

ISSN 0947-8620

urn:nbn:de:0005-069684

ANALYSE DER WASSERSTOFFPRODUKTION IN QUENCH VERSUCHEN

ZUSAMMENFASSUNG

Eines der Hauptziele des QUENCH-Vorhabens am Forschungszentrum Karlsruhe ist die Bestimmung des Wasserstoffquellterms beim Fluten eines überhitzten Reaktorkerns. Dafür werden verschiedene Methoden (Massenspektrometrie, Wärmeleitfähigkeit, Durchflussmessung, Bündelzustand nach dem Versuch) genutzt, um sowohl die Wasserstofffreisetzungsrate als auch die integrale Wasserstoffproduktion bei den komplexen und in der Abschreckphase hoch transienten Versuchen zu bestimmen.

Im vorliegenden Bericht werden die Ergebnisse aller bis Ende 2003 durchgeführten Versuche (QUENCH-01 bis QUENCH-09) einer kritischen Analyse unterworfen. Erstmals wurden in einer detaillierten Analyse Wasserstoffquellen den einzelnen oxidierten Bündelkomponenten zugeordnet.

Insgesamt ergeben die unterschiedlichen Auswertungsmethoden ein konsistentes Bild. Für einige Versuche mit großer Wasserstoffproduktion in der Abschreckphase werden geringfügige Korrekturen der Integralwerte für die Abschreckphase vorgeschlagen.

Dieser Bericht ergänzt und aktualisiert die bisher vorliegenden Datenberichte und FZKA-Berichte.

ABSTRACT

One of the main objectives of the QUENCH Program at FZK is the determination of the hydrogen source term during reflood of an overheated reactor core. For that reason different methods (mass spectrometry, heat conductivity, flow meter, post-test bundle status) are used to determine the hydrogen release rates as well as the integral hydrogen production during the complex and - during the quench phase - highly transient experiments.

A critical assessment of all bundle tests performed up to the end of 2003 is given. A detailed analysis of the post-test bundle status with attribution of hydrogen originating from the oxidation of the single bundle components is presented for the first time.

In general, consistent results are obtained with the various methods. Minor corrections are proposed for some tests with large hydrogen release during the quench phase.

This report complements and updates the data reports and FZKA reports published so far.

CONTENTS

LIST OF TABLES

LIST OF FIGURES

1 Introduction

The QUENCH program performed at FZK is to investigate the hydrogen source term and the bundle degradation during reflood of an overheated reactor core. The project consists of large scale bundle experiments, small-scale separate-effects tests, modelling activities as well as improvement, validation and application of SFD code systems.

The QUENCH Facility is a unique test facility with a 2.5 m long test bundle consisting of 21 electrically heated fuel rod simulators. It was brought into operation in 1997; nine tests have been performed so far. The facility and the tests have been described in detail elsewhere [1-7]; here only the hydrogen measurement is discussed.

The main gas analysis system is the quadrupole mass spectrometer Balzers GAM 300. Its sampling position is behinde orifice F601 in the off-gas pipe which results in short response times of less than 5 seconds.

In tests QU-04/05/06/07/09 a second, simpler mass spectrometer (Balzers Prisma) was used as a further check, which was located behind the steam condenser. The response times for this system were about 20-30 s and only non-condensable gases could be analysed.

A commercial-type hydrogen detection system CALDOS 7 G (Hartmann & Braun), also located behind the condenser at the end of the off-gas line, was additionally used in all tests. This system works on the basis of the thermal conductivity. It is calibrated for a binary Ar-H_2 gas mixture and delivers reliable data for standard tests without a B_4C absorber rod.

A 3D schematic view of the QUENCH facility with the positions of the different gas analysis systems is shown in Fig. 1.

Additionally, various indirect methods to evaluate the integral hydrogen release have been used, namely the off-gas flow meter F901 and the analysis of the amount of oxidised components from the post-test evaluation of the bundle (post-test bundle status PTBS).

This report compiles the results obtained with the different methods and gives recommendations for best-estimate hydrogen releases of all QUENCH tests performed so far. It complements and updates the FZKA reports given in the reference list.

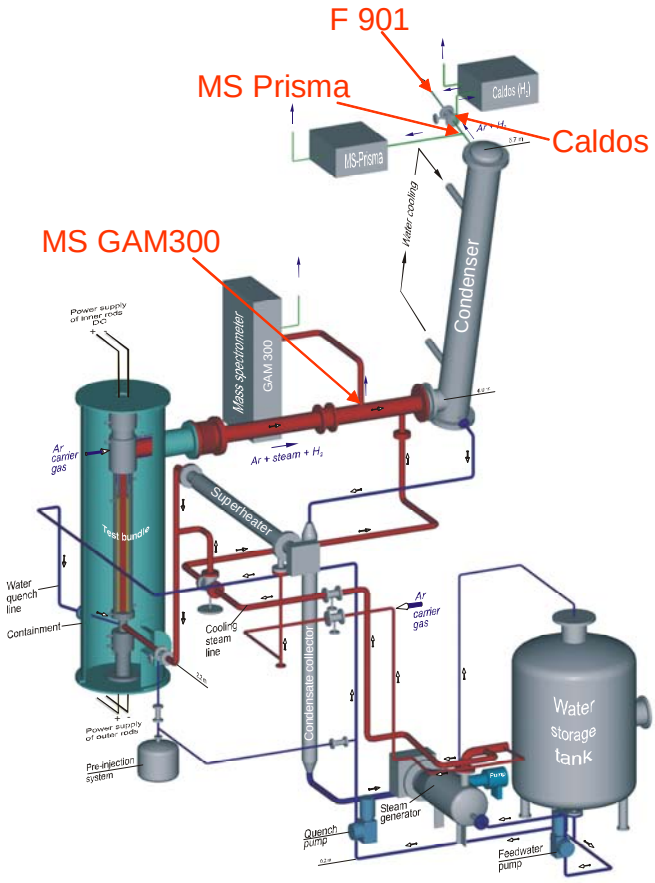

Fig. 1: 3D sketch of the QUENCH Facility with sampling positions for the mass spectrometers GAM300 and Prisma, the Caldos system and the off-gas flow meter F 901

2 Results of hydrogen release obtained with different methods

2.1 Mass spectrometer

The completely computer-controlled quadrupole mass spectrometer GAM300 (Balzers) is the main system for the analysis of hydrogen and other gases. The system has been working very reliably for several years. The QUENCH team also operates a second, very similar MS used for the separate-effects tests with excellent results.

Figure 2 shows the sampling position in the off-gas pipe behind orifice F601. The gas mixture is taken by a vertical tube with several holes directed to the gas flow from the test section in order to get a representative gas composition. The whole tube system from the sampling position to the mass spectrometer is heated to about 150 °C; therefore in principle steam concentration can be measured in addition to the non-condensing gases H_2, CO or N_2, O_2, CO_2, CH_4, Ar, Kr, He etc. (Problems in steam measurement due to partial condensation in the off-gas pipe are described in the appendix of [5].) Due to its position in the off-gas pipe the mass spectrometer GAM300 responds almost immediately to changes in the gas composition (response time <5 s).

The MS system GAM300 was improved several times. After test QU-01 the sampling position (Fig. 2) in the off-gas pipe was additionally heated to prevent condensation there; and, starting with test QU-06, an external source for steam calibration was installed. Up to test QU-07 a heat exchanger was installed between sampling position and MS, which was removed before test QU-09 because the off-gas temperature was below the safety limit of the MS in all preceding tests. This measure reduced the tube volume and thus the response time of the MS and made the system simpler. Furthermore, a heatable gas pump was installed between sampling position and MS before test QU-08. Previously, the driving force to transport the gas to the mass spectrometer was only the pressure gradient between test section (about 2 bar) and open atmosphere. The first two measures improved the quality of the steam measurement (and are thus not relevant for this paper); the last measure improved the general behaviour of the mass spectrometer especially during the highly transient quench phase.

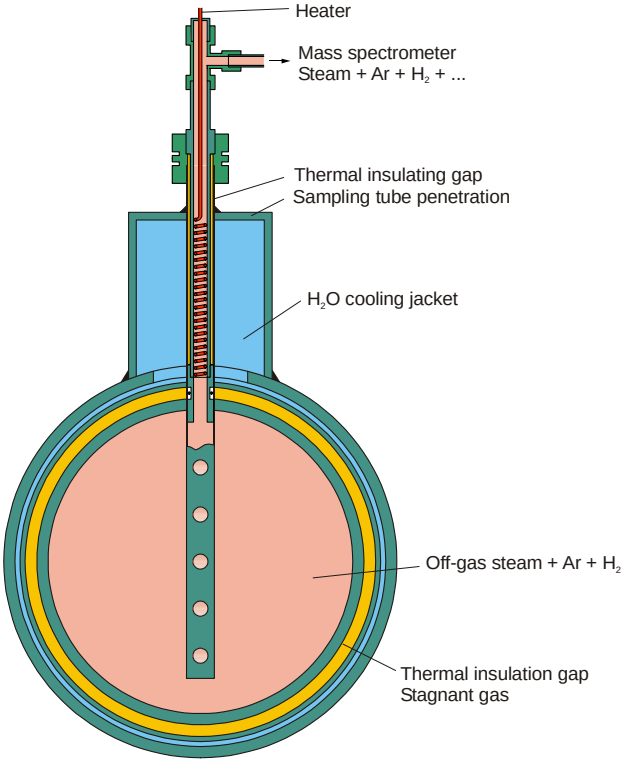

Fig. 2: Sampling position for the gases to be analysed by the MS GAM300 in the off-gas pipe of the facility behind the orifice F601

The mass spectrometer measures ion currents of the gas species to be analysed. These ion currents are transferred into volume concentrations by using a calibration factor matrix implemented in the MS software. The calibration factors of the non-condensable gases (including hydrogen) are determined with certified 95% Ar – 5% gas mixtures. Gas flow rates are calculated referring to the known mass flow rate of the reference gas argon based on Equ. 1.

$$\dot{m}_{H_2} = \frac{M_{H_2}}{M_{Ar}} \cdot \frac{C_{H_2}}{C_{Ar}} \cdot \dot{m}_{Ar} \qquad (1)$$

In some cases, for example where the Ar mass flow rate was not available or reliable, hydrogen mass flow rate was (partially) calculated referring to the steam mass flow rate (only

possible in the steam quenching tests QU-04/05/07/08/09). Then, Equ. 2 can be used taking into account the total steam injection and its partial consumption by the oxidation reaction.

$$\dot{m}_{H_2} = \frac{M_{H_2}}{M_{H_2O}} \cdot \frac{C_{H_2}}{C_{H_2} + C_{H_2O}} \cdot \dot{m}_{H_2O} \qquad (2)$$

Figure 3 summarises input flow rates of argon, steam and water; concentrations of hydrogen, argon and steam measured by MS and the calculated hydrogen release rate for all QUENCH experiments conducted so far. Special subjects of interest in these diagrams are the maximum hydrogen concentrations before and during the quench phase, and the minimum argon concentration during the quench phase. If the latter is very low, large errors in the calculations of the hydrogen mass flow rates (C_{Ar} in the denominator of Equ.1!) have to be expected.

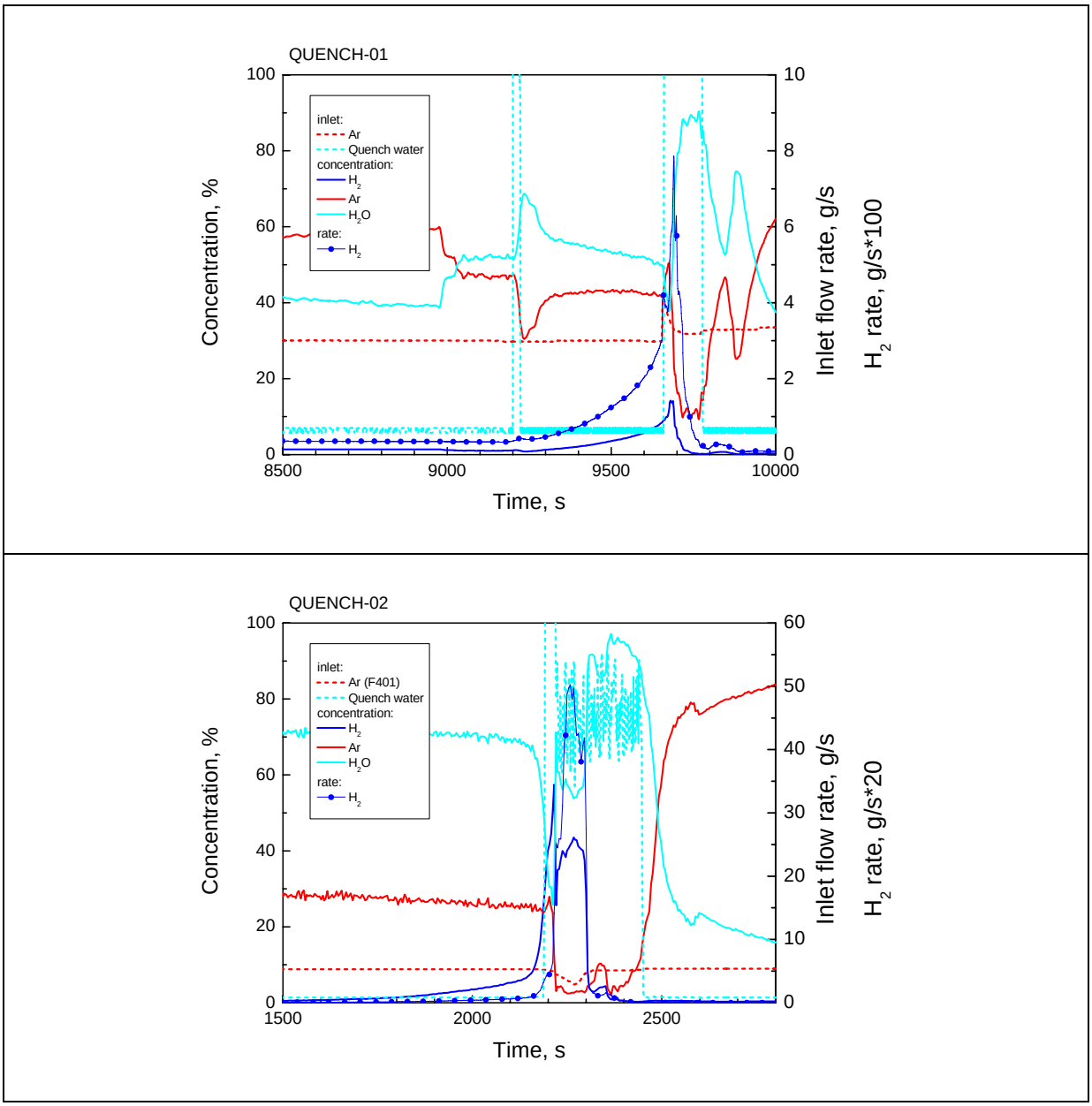

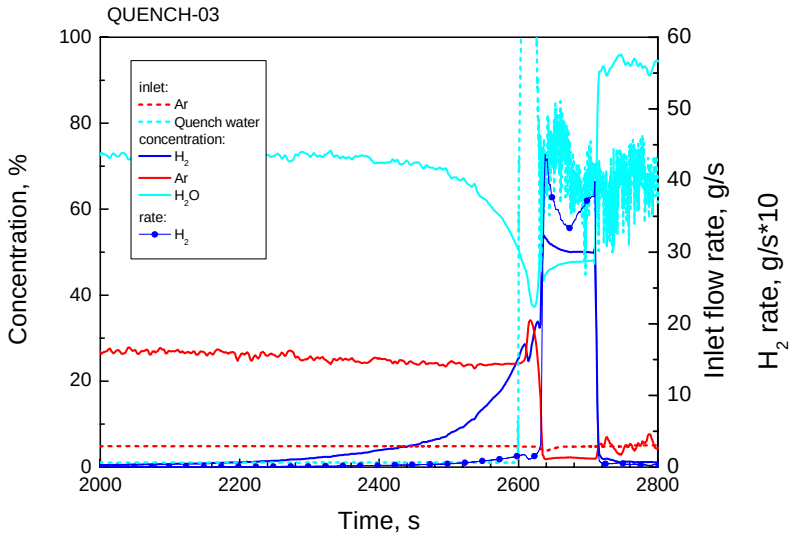
QUENCH-03
inlet:
Ar
Quench water
concentration:
H2
Ar
H2O
rate:
H2
Concentration, %
Inlet flow rate, g/s
H2 rate, g/s*10
Time, s

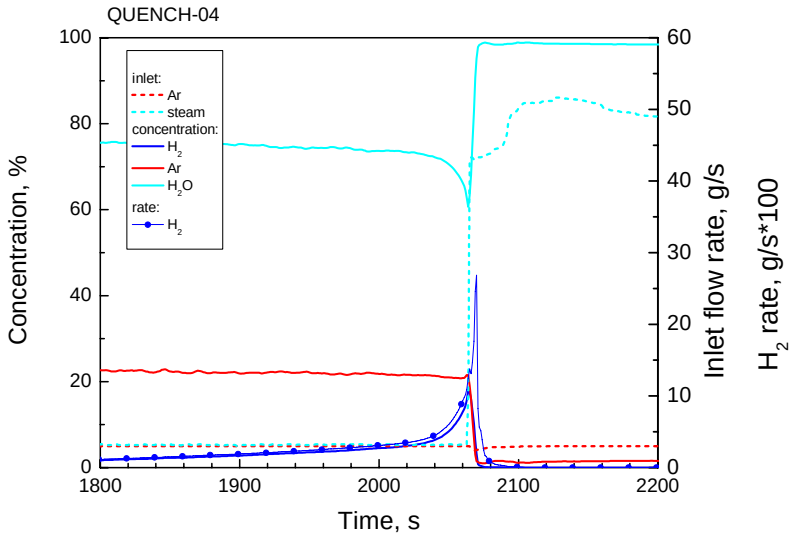
QUENCH-04
inlet:
Ar
steam
concentration:
H2
Ar
H2O
rate:
H2
Concentration, %
Inlet flow rate, g/s
H2 rate, g/s*100
Time, s

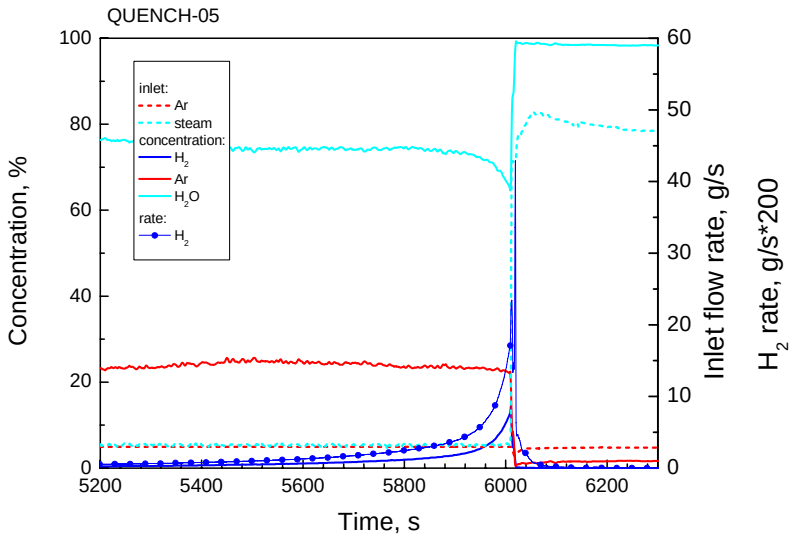
QUENCH-05
inlet:
Ar
steam
concentration:
H2
Ar
H2O
rate:
H2
Concentration, %
Inlet flow rate, g/s
H2 rate, g/s*200
Time, s

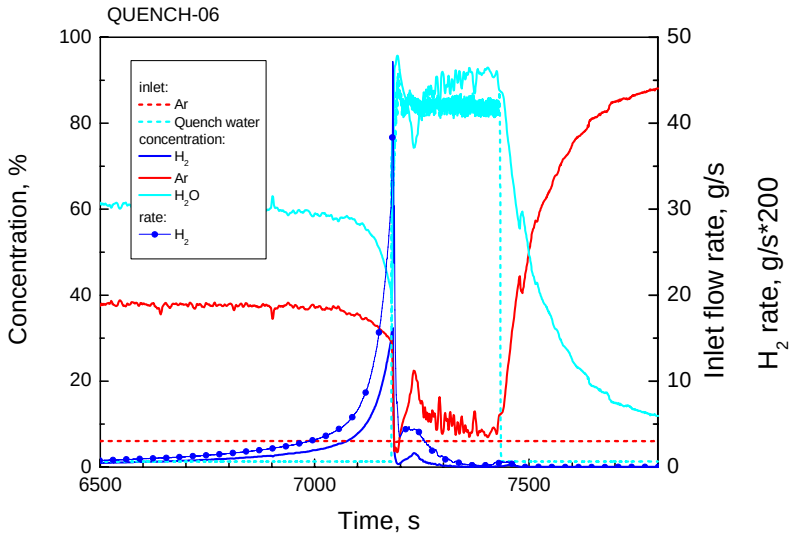
QUENCH-06
inlet:
Ar
Quench water
concentration:
H2
Ar
H2O
rate:
H2
Concentration, %
Inlet flow rate, g/s
H2 rate, g/s*200
Time, s

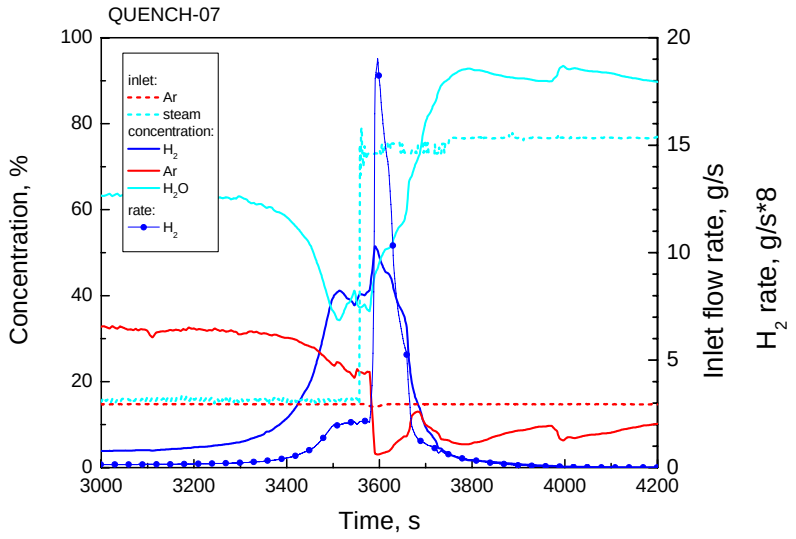
QUENCH-07
inlet:
Ar
steam
concentration:
H2
Ar
H2O
rate:
H2
Concentration, %
Inlet flow rate, g/s
H2 rate, g/s*8
Time, s

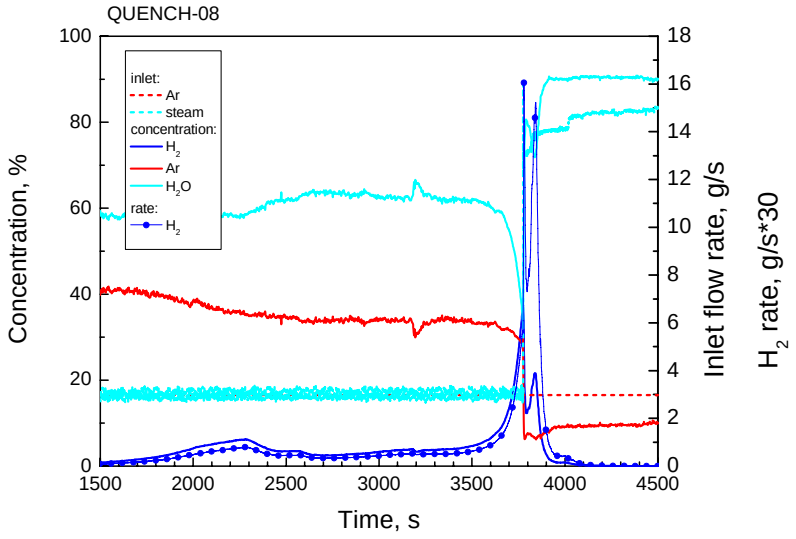
QUENCH-08
inlet:
Ar
steam
concentration:
H2
Ar
H2O
rate:
H2
Concentration, %
Inlet flow rate, g/s
H2 rate, g/s*30
Time, s

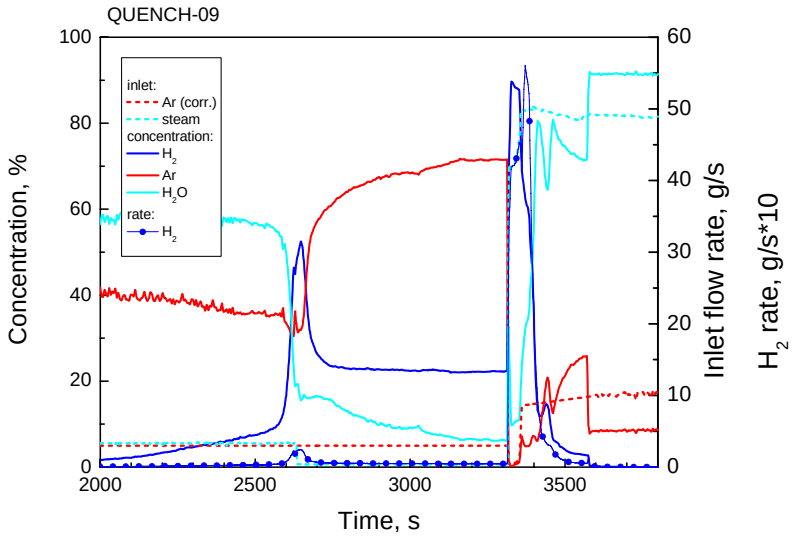

Fig. 3: Inlet flow rates of argon, steam and water; concentrations of hydrogen, argon and steam measured by MS, and calculated hydrogen release rate for all QUENCH experiments conducted till 12/03

During the quench phase of test QU-03 the gas flow to the mass spectrometer was blocked after initiation of reflood for about 80 s, so that the gas was stagnant in the analyser for that time. Therefore, the MS data are only reliable up to the end of the transient phase and are overestimated for the quench phase.

Especially in the test QU-09, the argon concentration was almost zero for about 30 s in the quench phase. Furthermore, the cooling jacket failed 27 s after initiation of the quench phase leading to an argon flow from the cooling system into the bundle, so that m_{Ar} was unknown. Therefore, the argon rate was re-evaluated using the steam injection data from the beginning of the quench phase.

Evaluation of the MS data referred to argon and steam and of a combination of both, namely based on Ar before and on steam during the quench phase, is given in Table 3. Additionally, results obtained with the second mass spectrometer Prisma are given in this table. They have to be regarded as less reliable than the GAM300 due to a strong dependence of the results on system pressure which had to be corrected in the evaluation of the data.

The results obtained with the Prisma system were strongly dependent on system pressure. They had to be re-evaluated after the tests and are considered to be of a limited reliability.

2.2 Caldos system

The principle of measurement of the Caldos system is based on the different heat conductivities of different gases. The Caldos device is calibrated for the hydrogen-argon gas mixture. To avoid any moisture in the analyzed gas, a gas cooler, which is controlled at 296 K, is connected to the gas analyzer. The response time of the gas analyzer is documented by the manufacturer to be 2 s, i.e. a time in which 90 % of the final value should

be reached. Due to its position behind the condenser the real delay time is about 20-30 s. In contrast to the mass spectrometer the Caldos device only measures the hydrogen content.

With an argon-hydrogen (two-component) mixture that in fact exists at the location of the Caldos analyzer Equ. 1 can be written as follows

$$\dot{m}_{H_2} = \frac{M_{H_2}}{M_{Ar}} \cdot \frac{C_{H_2}}{100 - C_{H_2}} \cdot \dot{m}_{Ar} \tag{3}$$

The Caldos system (Fig. 4) was upgraded after test QU-03 with respect to its delay time. The void volume of the inlet line of the Caldos system was reduced and an additional pump was added in a bypass to the existing pump. With these modifications the delay time was reduced from 100 s to approx. 20 s.

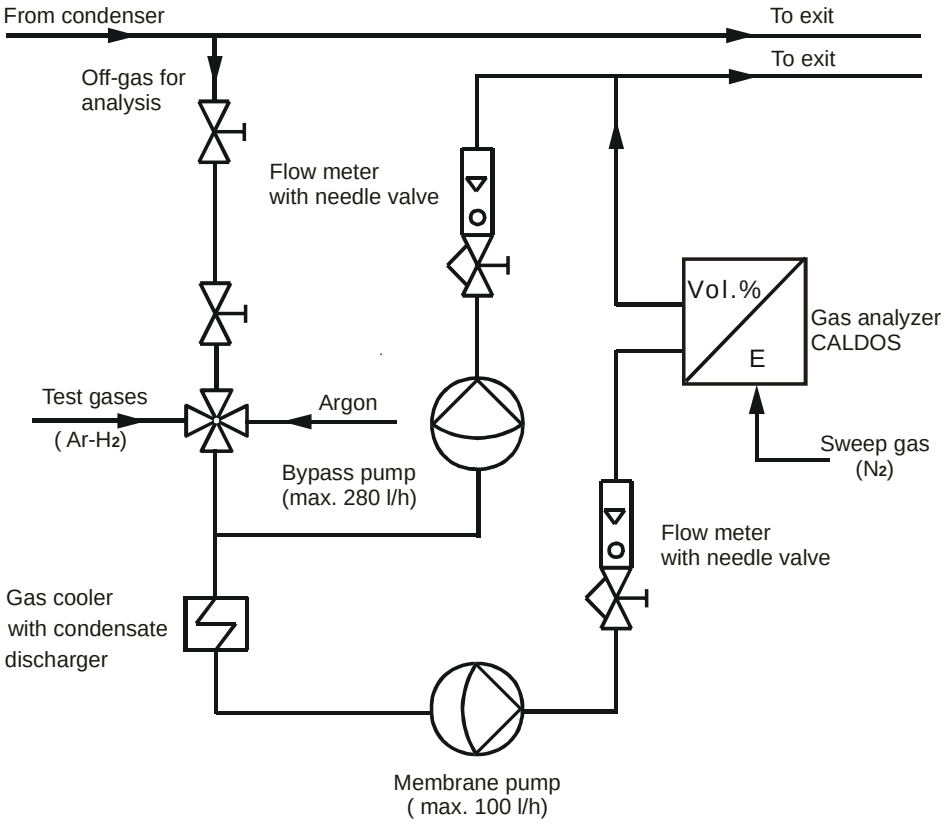

Fig. 4: Hydrogen measurement with the CALDOS analyzer connected to the exhaust gas pipe of the QUENCH facility

The data obtained by the Caldos system are also compiled in Table 3. Data for test QU-02 are not available because of a failure of the main data acquisition system. The results of test QU-03 are not reliable because the gas sampling was too slow in the highly transient quench phase. For the experiments QU-07/09 with boron carbide central rod the Caldos system can't deliver reliable data because of its calibration for a particular binary gas mixture and was only operated for qualitative evaluation of the gas release.

2.3 Off-gas flow meter F901

After the unsatisfactory results with respect to the gas analysis of test QU-03 the data of the off-gas flow meter F901 behind the main condenser were used to estimate the hydrogen release in the quench phase. The total mass flow was calculated using Equ. 4, given by the supplier of the facility (Siemens).

$$\dot{m} = 10.45 \cdot \dot{V}_{meas} \cdot \sqrt{\frac{p \cdot \rho_N}{T}} \cdot \frac{1000}{3600} \qquad (4)$$

with $\dot{m}$ gas mass flow rate in g/s, $\dot{V}_{meas}$ measuring signal F901 in m^3/h, p absolute pressure P901 in bar, T temperature in K and ρ_N gas density under normal conditions in kg/m^3 (0.09 for H_2).

The base line of the curve obtained with Equ. 4 was shifted to zero to eliminate the 3 g/s argon gas. For the evaluation of the cumulated hydrogen mass, the signal was integrated, but only for the quench phase and the value was added to that obtained by the more precise MS up to the end of the transient phase. The following integration boundaries were applied for the three tests.

QU-01: $\int_0^{9682} \dot{m}_{H_2} dt + \int_{9683}^{9769} FM901 dt$

QU-02: $\int_0^{2199} \dot{m}_{H_2} dt + \int_{2200}^{2322} FM901 dt$

QU-03: $\int_0^{2619} \dot{m}_{H_2} dt + \int_{2620}^{2671} FM901 dt$

The flow meter F901 was only available in tests QU-01/02/03; in later tests it was bypassed due to technical reasons.

The results of the F901 analyses are included in Table 3. The value for QU-01 is significantly higher than the consistent values of the MS, Caldos and the value obtained from the post-test bundle status (see below), thus showing the relatively high inaccuracy of the procedure. On the other hand, this method delivers reasonable values for tests QU-02/03 with higher hydrogen release rates in the quench phase.

The value given for QU-02 (167 g) differs from that given in the report FZKA-6295 (123 g) due to a more accurate evaluation of the data taking into account the actual values of P601 and T601 (instead of mean values) and a corrected shift of the data for the argon gas elimination.

2.4 Post-test bundle status

A complementary method for the evaluation of the integral hydrogen release is the analysis of the oxidised components of the bundle and its conversion into hydrogen production. An extensive evaluation of all oxidisable components was done taking separately into account

cladding tubes, corner rods, shroud, grid spacers, tungsten heaters, molybdenum electrodes, high-temperature thermocouples, boron carbide (absorber rods) and oxidised melt.

The following chemical equations for the interaction between steam and metal or B_4C were used taking into account complete oxidation of the metals:

$$Zr + 2H_2O \Leftrightarrow ZrO_2 + 2H_2 \quad (5)$$

$$W + 3H_2O \Leftrightarrow WO_3 + 3H_2 \quad (6)$$

$$Mo + 3H_2O \Leftrightarrow MoO_3 + 3H_2 \quad (7)$$

$$2Ta + 5H_2O \Leftrightarrow Ta_2O_5 + 5H_2 \quad (8)$$

$$B_4C + 7.5H_2O \Leftrightarrow 2B_2O_3 + 0.5CO + 0.5CO_2 + 7.5H_2 \quad (9)$$

$$3Fe + 4H_2O \Leftrightarrow Fe_3O_4 + 4H_2 \quad (10)$$

In the following, the equations for the conversion of oxidised components into hydrogen production for the various components are given. They are based either on the oxide scale volume in case of partial oxidation (i.e. oxide scale on metal layer) or on consumed metal or B_4C in case of complete oxidation. The description of variables and constants as well as their values are given in Table 1 at the end of this chapter.

The axial integral ZrO_2 thicknesses of cladding tubes (mean value), corner rods and shroud is calculated using the data from the Test Data Reports and the FZKA Reports. Missing data are interpolated or extrapolated. Oxide scale thicknesses of grid spacers and TC sheaths are assumed to be the same as the mean cladding values unless they are directly available. The oxidation of tungsten heaters and molybdenum electrodes is estimated by interpolation and extrapolation of available diameters from the metallographic cross sections.

2.4.1 Cladding tubes

The normally-used 21 cladding tubes are exposed to the steam atmosphere over a length of about 1965 mm (from -470 mm to 1495 mm bundle elevation). The fuel rod simulators are heated over a length of 1024 mm (from 0 mm to 1024 mm). Maximum temperatures and thus maximum oxidation is obtained in the upper part of the bundle at about 950 mm.

The following formulae were used to calculate the mass of hydrogen evolved from the cladding steam oxidation

a) for partial oxidation:

$$m_{H_2}^{clad} = 21 \cdot \pi \cdot \int d_{ox} dx \cdot D_{clad} \cdot \rho_{ZrO_2} \cdot \frac{2M_{H_2}}{M_{ZrO_2}} \cdot \alpha = 15.5 \cdot \int d_{ox} dx \quad (11)$$

for tests with unheated central rod, and

$$m_{H_2}^{clad} = 20 \cdot \pi \cdot \int d_{ox} dx \cdot D_{clad} \cdot \rho_{ZrO_2} \cdot \frac{2M_{H_2}}{M_{ZrO_2}} \cdot \alpha = 14.8 \cdot \int d_{ox} dx \quad (11a)$$

for tests with absorber rod; these are considered separately in Equs. 26-28.

b) for complete oxidation per cm and tube:

$$m_{H_2}^{clad} = \pi \cdot (D_{clad} - d_{clad}) \cdot d_{clad} \cdot \rho_{Zr} \cdot \frac{2M_{H_2}}{M_{Zr}} = 0.065 \quad (12)$$

where d_{ox} is the mean oxide layer thickness at height x, D_{clad} is the outer cladding diameter and α is the factor to allow for α-Zr(O) formation (see Table 1).

2.4.2 Corner rods

Four corner rods are installed in the bundle in order to prevent artificially large flow channels between the bundle and the shroud in these positions. Three of them are used for additional TC instrumentation at elevations 550, 850, and 950 mm. They consist of solid rods from the TC position up to the upper end at 1300 mm and of tubes for the TC wires from the bottom to the elevation of the TC probe. The fourth rod is foreseen to be removed during the test, usually at about the end of the pre-oxidation and before the quench phase. It ranges up to 1155 mm bundle elevation.

The formulae used for H_2 evolution from the corner rods are then the following (D_{CR} and d_{CR} replace D_{clad} and d_{clad})

a) for partial oxidation:

$$m_{H_2}^{CR} = 4 \cdot \pi \cdot \int d_{ox} dx \cdot D_{CR} \cdot \rho_{ZrO_2} \cdot \frac{2M_{H_2}}{M_{ZrO_2}} \cdot \alpha = 1.65 \cdot \int d_{ox} dx \quad (13)$$

b) for complete oxidation per cm and tube:

$$m_{H_2}^{CR} = \pi \cdot (D_{CR} - d_{CR}) \cdot d_{CR} \cdot \rho_{Zr} \cdot \frac{2M_{H_2}}{M_{Zr}} = 0.045 \quad (14)$$

c) for complete oxidation per cm and full rod:

$$m_{H_2}^{CR} = \pi \cdot \frac{D_{CR}^2}{4} \cdot \rho_{Zr} \cdot \frac{2M_{H_2}}{M_{Zr}} = 0.081 \quad (15)$$

2.4.3 Shroud inner surface

The shroud encloses the bundle from elevation -300 mm to 1300 mm. The corresponding formulae are:

a) for partial oxidation:

$$m_{H_2}^{shr} = \pi \cdot \int d_{ox} dx \cdot D_{shr} \cdot \rho_{ZrO_2} \cdot \frac{2M_{H_2}}{M_{ZrO_2}} \cdot \alpha = 5.48 \cdot \int d_{ox} dx \quad (16)$$

b) for complete oxidation per cm:

$$m_{H_2}^{shr} = \pi \cdot (D_{shr} - d_{shr}) \cdot d_{shr} \cdot \rho_{Zr} \cdot \frac{2M_{H_2}}{M_{Zr}} = 1.76 \quad (17)$$

2.4.4 Grid spacers

Five grid spacers are located at elevations -200, 50, 550, 1050, and 1410 mm. They are made of Zircaloy-4 except for the lowest which is made of Inconel alloy. For oxidation only the three upper grid spacers have to be considered because oxide scales at elevations -200 and 50 mm are negligible. The formulae are:

a) for partial oxidation:

$$m_{H_2}^{GS} = 2 \cdot h_{GS} \cdot l_{GS} \cdot d_{ox} \cdot \rho_{ZrO_2} \cdot \frac{2M_{H_2}}{M_{ZrO_2}} \cdot \alpha = 132 \cdot d_{ox} \quad (18)$$

b) for complete oxidation per grid spacer:

$$m_{H_2}^{GS} = h_{GS} \cdot l_{GS} \cdot d_{GS} \cdot \rho_{Zr} \cdot \frac{2M_{H_2}}{M_{Zr}} = 4.3 \quad (19)$$

2.4.5 Tungsten heaters

Tungsten heaters are installed in all fuel rod simulators at elevation 0-1024 mm for electrical heating of the bundle except for the central one which is used for additional instrumentation or absorber rods. They are surrounded by annular ZrO_2 pellets and are usually not in contact with steam. Only during tests with very severe degradation of the bundle (so far only QU-09) they can be partly oxidised. In this case, it is assumed that the consumed tungsten is completely oxidised according to Equ. 6 (and not relocated in eutectic metal mixtures).

The formula for hydrogen evolution by the oxidation of tungsten is:

$$m_{H_2}^{W} = n \cdot \varepsilon \cdot \pi \cdot l_W \cdot \frac{D_W^2}{4} \cdot \rho_W \cdot \frac{3M_{H_2}}{M_W} = 0.178 \cdot n \cdot \varepsilon \cdot l_W \quad (20)$$

$$\text{where } \varepsilon = 1 - \left(\frac{D_{post-test}}{D_{pre-test}} \right)^2 \quad (21)$$

2.4.6 Molybdenum electrodes

Molybdenum electrodes are used between tungsten heaters and the outer copper electrodes. They can be oxidised during tests with severe escalations in the upper part of the bundle where they are present from 1024 mm to 1600 mm elevation. Missing electrode material is assumed to be completely oxidised according to Equ. 7 similarly to tungsten. Only for test QU-09, where 15 Mo electrodes were missing over a length of about 30 cm, this part is assumed to be only partly oxidised (50%) because a certain amount of Mo is found in the melt pools.

The formula used for H_2 due to Mo oxidation of n rods is then:

$$m_{H_2}^{Mo} = n \cdot \varepsilon \cdot \pi \cdot l_{Mo} \cdot \frac{D_{Mo}^2}{4} \cdot \rho_{Mo} \cdot \frac{3M_{H_2}}{M_{Mo}} = 0.371 \cdot n \cdot \varepsilon \cdot l_{Mo} \quad (22)$$

where ε is the estimated fraction of metal oxidised.

2.4.7 HT thermocouples

The high-temperature thermocouples consist of a Zircaloy-4 external and a tantalum internal sheath. About 18 such thermocouples are laid through to the hot zone of the bundle. Their contribution to the total hydrogen release is relatively low (see table 2); therefore they are collectively treated as n=18/2=9 thermocouples which takes into account their length either from the bottom or from the top of the bundle. The formulae for H_2 evolution due to the HT thermocouple oxidation are as follows:

a) for partial oxidation of Zry-4 external sheath:

$$m_{H_2}^{TCZ} = n \cdot \pi \cdot \int d_{ox} dx \cdot D_{TCZ} \cdot \rho_{ZrO_2} \cdot \frac{2M_{H_2}}{M_{ZrO_2}} \cdot \alpha = n \cdot 0.12 \cdot \int d_{ox} dx \quad (23)$$

b) for complete oxidation of Zry-4 external sheath for a length l:

$$m_{H_2}^{TCZ} = n \cdot l \cdot \pi \cdot \left(D_{TCZ} - d_{TCZ}\right) \cdot d_{TCZ} \cdot \rho_{Zr} \cdot \frac{2M_{H_2}}{M_{Zr}} = 0.0055 \cdot n \cdot l \quad (24)$$

c) for complete oxidation of Ta internal sheath:

$$m_{H_2}^{TCT} = n \cdot l \cdot \pi \cdot \left(D_{TCT} - d_{TCT}\right) \cdot d_{TCT} \cdot \rho_{Ta} \cdot \frac{5M_{H_2}}{2M_{Ta}} = 0.0039 \cdot n \cdot l \quad (25)$$

2.4.8 B_4C absorber rod

The control rods used in tests QU-07 and QU-09 consisted of a boron carbide pellet stack in the heated zone of the bundle, stainless steel cladding and Zircaloy-4 guide tube. The amount of B_4C oxidised due to Equ. 9 has been estimated from the post-test bundle status, assuming complete oxidation of the missing material. The formulae for the hydrogen evolution are as follows:

a) for complete oxidation of pellet stack with length l:

$$m_{H_2}^{B_4C} = \pi \cdot \frac{D_{B_4C}^2}{4} \cdot l_{B_4C}^{ox} \cdot \rho_{B_4C} \cdot \frac{7.5M_{H_2}}{M_{B_4C}} = 0.214 \cdot l_{B_4C}^{ox} \quad (26)$$

b) for complete oxidation of SS cladding tube:

$$m_{H_2}^{SS} = l \cdot \pi \cdot \left(D_{SS} - d_{SS}\right) \cdot d_{SS} \cdot \rho_{Fe} \cdot \frac{4M_{H_2}}{3M_{Fe}} = 0.134 \cdot l \quad (27)$$

c: for complete oxidation of Zry-4 guide tube

$$m_{H_2}^{CRZ} = l \cdot \pi \cdot \left(D_{CRZ} - d_{CRZ}\right) \cdot d_{CRZ} \cdot \rho_{Zr} \cdot \frac{2M_{H_2}}{M_{Zr}} = 0.042 \cdot l \quad (28)$$

2.4.9 Oxidised melt

Only a rough estimation of the volume of oxidised melt is possible from the metallographic post-test examination. It is only taken into account when it could be assumed that it does not originate from other parts of the bundle where it has already been considered (e.g. by complete oxidation of this region). The formula used for hydrogen generation from melt oxidation was then:

$$m_{H_2}^{melt} = V_{melt}^{ox} \cdot \rho_{melt} \cdot \frac{2M_{H_2}}{M_{ZrO_2}} = 0.032 \cdot V_{melt}^{ox} \cdot \rho_{melt} \quad (29)$$

Table 1: Variables and constants for the calculation of hydrogen production due to the oxidation of the various bundle components

variable/constant	value	unit	description
m_{H2}		g	hydrogen mass produced by the oxidation of the component (indicated in the superscript) by steam
d_{ox}		cm	oxide scale thickness
n			number of rods, TCs etc. partially or wholly oxidised
x		cm	axial elevation
D_{clad}	1.075	cm	outer diameter of cladding tube
D_{CR}	0.6	cm	outer diameter of corner rod
D_{shr}	8	cm	inner diameter shroud
D_W	0.6	cm	diameter of W heater rod
D_{Mo}	0.86	cm	diameter of Mo electrode
D_{TCZ}	0.21	cm	outer diameter of outer Zry-4 TC sheath
D_{TCT}	0.14	cm	outer diameter of inner Ta TC sheath
D_{B4C}	0.747	cm	diameter of B4C pellet stack
D_{SS}	1.024	cm	diameter of SS cladding of absorber rod
D_{CRZ}	1.21	cm	outer diameter of Zry-4 CR guide tube
d_{clad}	0.0725	cm	cladding wall thickness
d_{CR}	0.1	cm	corner tube wall thickness
d_{shr}	0.238	cm	shroud wall thickness
d_{TCZ}	0.035	cm	HT-TE Zry-4 sheath thickness
d_{TCT}	0.023	cm	HT-TE Ta sheath thickness

d_{SS}	0.126	cm	SS cladding thickness of absorber rod
d_{CRZ}	0.04	cm	Zry-4 guide tube thickness of absorber rod
h_{GS}	4.2	cm	height of Zry-4 grid spacers
l_{GS}	72	cm	total length of Zry-4 grid spacer sheets
d_{GS}	0.05	cm	thickness of Zry-4 grid spacers
l_W		cm	length of oxidised region of W heater
l_{Mo}		cm	length of oxidised region of Mo electrode
l_{B4C}^{ox}		cm	length of completely oxidised B_4C pellet stack
V_{melt}^{ox}		cm^3	estimated volume of oxidised melt (ZrO_2)
ρ_{Zr}	6.5	g/cm^3	density of zirconium
ρ_{ZrO2}	5.6	g/cm^3	density of ZrO_2
ρ_W	19.3	g/cm^3	density of tungsten
ρ_{Mo}	10.2	g/cm^3	density of molybdenum
ρ_{Ta}	16.5	g/cm^3	density of tantalum
ρ_{B4C}	1.8	g/cm^3	density of B_4C
ρ_{Fe}	7.9	g/cm^3	density of Fe (as main component of SS)
ρ_{melt}	~4	g/cm^3	estimated density of porous zirconia melt
M_{H2}	2	g/mol	molar mass of H_2
M_{Zr}	91.2	g/mol	molar mass of Zr
M_{ZrO2}	123.2	g/mol	molar mass of ZrO_2
M_W	184	g/mol	molar mass of W
M_{Mo}	95.9	g/mol	molar mass of Mo
M_{Ta}	180.9	g/mol	molar mass of Ta
M_{B4C}	55.25	g/mol	molar mass of B_4C
M_{Fe}	55.85	g/mol	molar mass of Fe (as main component of SS)
α	1.2		+ 20% H_2 production due to the formation of α-Zr(O)
ε			estimated fraction of metal (W, Mo) oxidised
$D_{pre\text{-}test}$			original diameter (of W, Mo rods)
$D_{post\text{-}test}$			diameter of degraded (W, Mo) rods after test

2.4.10 Summary of post-test bundle evaluation

Table 2 compiles the results of the calculations done with Equs. 11-29 for all QUENCH bundle experiments. Additionally, the integral value for each test is given in Table 3.

The hydrogen production data obtained by the evaluation of the post-test bundle status support the data obtained by the MS. Therefore, for test QU-03, where MS data are unreliable for the quench phase (see above), post-test bundle values can be taken as a basis for evaluation. The difference between MS data and post-test evaluation data is less than 20 % for all other tests.

The hydrogen mass originating from oxidation of prototypic bundle components excluding shroud, thermocouples, heaters and electrodes is given in the last column of Table 2. This value is about 80 % for the tests without escalation and around 70 % for the test with escalation except for the most severe test QU-09 where only 38 % of the hydrogen is produced by the oxidation of cladding, corner rods, grid spacers, and absorber rod. Most of the hydrogen is produced by the oxidation of the cladding tubes in all tests except for QU-09 where the heavy oxidation of the shroud caused the main hydrogen release.

3 Discussion, summary and conclusions

The determination of the hydrogen source term during reflood of an overheated reactor core is one of the main objectives of the QUENCH Program. Thus, it is important to have reliable data on the release of hydrogen during the QUENCH bundle tests and especially for the highly transient quench or cooling phases.

In this report, different direct and indirect methods for the analysis of hydrogen release are compiled. A detailed analysis of the oxidised components from the post-test bundle status for all tests as well as the analyses of the FM901 off-gas flow signal for tests QU-01/03 are performed for the first time. Additionally, the FM901 evaluation for test QU-02 has been re-evaluated.

A very consistent data set exists for all tests with no temperature escalation during the quench phase (QU-01/04/05/06) and for the test QU-08 with moderate excursion. There is no need to propose corrections for these experiments.

Additionally, the MS GAM300 data are known to be reliable in all phases before quenching. In consequence, the following conclusions can be drawn for the tests with temperature escalation.

The hydrogen release measured by the MS GAM300 during the quench phase in test QU-02 is probably slightly overestimated. According to the data from FM901 and post-test bundle status (PTBS) it is proposed to reduce the value from 170 to 140 g (see Table 3).

For test QU-03 only FM901 and PTBS data are available and 120 g H_2 released during the quench phase is proposed as best-estimate value.

For tests QU-07 and QU-09 the data obtained by the mass spectrometer are generally verified by the PTBS evaluation. MS analysis based on steam injection flow rates and PTBS indicate slightly lower values than the GAM300 standard analysis based on argon as reference gas. So, best-estimate values for hydrogen release in the quench phase in these tests are given as 120 and 400 g, respectively.

The PTBS analysis for test QU-08 correlates very well with the data obtained by MS and Caldos measurements. Obviously, the installation of a gas pump before this test improved the performance of the MS measurement especially during the highly transient quench phase.

The analyses given in this report considered only the integral hydrogen release during the quench bundle tests. No changes are proposed for the rates given in the earlier FZKA reports. Again, one can say, that the hydrogen release rates measured by the MS GAM300 can be regarded as reliable. The maximum H_2 release rate measured during the quench phase should be reliable, too. Only the course of the hydrogen rates should be taken with care due to the highly transient character of the quench phase especially for the tests with temperature escalation.

Altogether, this work clearly supports the subdivision of the tests in those with temperature and thus hydrogen escalation in the quench phase and those with immediate cooldown (successful reflood) and low H_2 release with initiation of the quench phase. The heat balance

at initiation of reflood is the decisive criteria for the success of flooding the overheated bundle. Furthermore, tests QU-07/08/09 provide good indications of the influence of boron carbide control rods and steam starvation conditions on the course and intensity of the temperature excursion. This is supported by separate-effect test results, but it has to be confirmed by further code calculations.

4 References

[1] P. Hofmann, W. Hering, C. Homann, W. Leiling, A. Miassoedov, D. Piel, L. Schmidt, L. Sepold, M. Steinbrück, “QUENCH-01, Experimental and Calculational Results,” FZKA 6100, Forschungszentrum Karlsruhe, 1998.

[2] P. Hofmann, C. Homann, W. Leiling, A. Miassoedov, D. Piel, G. Schanz, L. Schmidt, L. Sepold, M. Steinbrück, “Experimental and Calculational Results of the Experiments QUENCH-02 and QUENCH-03,” FZKA 6295, Forschungszentrum Karlsruhe, 2000.

[3] L. Sepold, P. Hofmann, C. Homann, W. Leiling, A. Miassoedov, D. Piel, G. Schanz, L. Schmidt, U. Stegmaier, M. Steinbrück, H. Steiner, “Investigation of an Overheated PWR-Type Fuel Rod Simulator Bundle Cooled Down by Steam. Experimental and Calculational Results of the QUENCH-04 Test,” FZKA 6412, Forschungszentrum Karlsruhe, 2002.

[4] L. Sepold, C. Homann, W. Leiling, A. Miassoedov, D. Piel, G. Schanz, L. Schmidt, U. Stegmaier, M. Steinbrück, H. Steiner, “Experimental and Calculational Results of the QUENCH-05 Test,” FZKA 6615, Forschungszentrum Karlsruhe, 2002.

[5] L. Sepold, C. Homann, A. Miassoedov, G. Schanz, U. Stegmaier, M. Steinbrück, H. Steiner, J. Stuckert, “Experimental and Calculational Results of the QUENCH-06 Test (OECD ISP-45),” FZKA 6664, Forschungszentrum Karlsruhe, 2004.

[6] M. Steinbrück, C. Homann, A. Miassoedov, G. Schanz, L. Sepold, U. Stegmaier, H. Steiner, J. Stuckert, “Results of the B_4C Control Rod Test QUENCH-07,” FZKA 6746, Forschungszentrum Karlsruhe, 2004.

[7] M. Steinbrück, C. Homann, A. Miassoedov, G. Schanz, L. Sepold, U. Stegmaier, H. Steiner, J. Stuckert, “Results of the QUENCH-09 Experiment with a B_4C Control Rod,” FZKA 6829, Forschungszentrum Karlsruhe, 2004.

5 Acknowledgements

The author is grateful to Ulrike Stegmaier who did a great job in post-test metallography of the bundles. Furthermore, I want to thank Christoph Homann, Gerhard Schanz, Leo Sepold, and Juri Stuckert (all FZK) for the fruitful discussions during the preparation of this report. Finally, I thank David Bottomley (ITU) for the careful review of the report.

Table 2: Integral hydrogen production (in g) based on post-test analysis of oxidation of bundle components

Test	Cladding	Corner rod	Shroud	Grid spacer	HT-TC Zry-4	HT-TC Ta	W heater	Mo electrode	B_4C (+SS+Zry)	Melt*	Σ all	Clad, CR, GS, B_4C, melt
QU-01	23	2	5	2	2	-	-	-	-	-	**34**	**27**
QU-02	69	8	20	5	2	1	-	28	-	19	**152**	**101**
QU-03	75	6	27	5	2	1	-	14	-	5	**135**	**91**
QU-04	10	1	2	1	1	-	-	-	-	-	**14**	**12**
QU-05	18	2	4	3	1	-	-	-	-	-	**28**	**23**
QU-06	25	2	6	3	2	-	-	-	-	-	**37**	**30**
QU-07	89	10	23	8	3	1	-	22	4+3+1	13	**177**	**128**
QU-08	57	5	15	5	3	-	-	-	-	-	**85**	**67**
QU-09	132	22	169	13	5	3	23	100	10+7+2	-	**486**	**186**

** Oxidised melt not considered during evaluation of the various components*

Table 3: Integral hydrogen production (in g) based on various evaluation methods

Test	MS GAM300 ref. to Ar	MS GAM ref. to steam	$t<t_{quench}$: Ar $t>t_{quench}$: H_2O	MS Prisma	Caldos	FM901	PTBS	$\frac{GAM300 - PTBS}{PTBS}$	Best estimate before[a] / during quench phase
QU-01	39	-	-	-	35	55	34	0.13	36 / 3
QU-02	190	-	-	-	-	169	152	0.2	20 / 140
QU-03	(288)[b]	-	-	-	(47)[b]	167	135	-	18 / 120
QU-04	12	11	14	11	12	-	14	-0.17	10 / 2
QU-05	27	23	28	28	27	-	28	-0.04	25 / 2
QU-06	36	-	-	42	35	-	37	-0.03	32 / 4
QU-07	198	164	151	201	(148)[b]	-	177	-0.11	62 / 120
QU-08	84	82	75	-	92	-	85	-0.01	46 / 38
QU-09	468	448	459	(59)[b]	(113)[b]	-	486	-0.04	60 / 400

a - MS GAM300 data

b - Unreliable data due to known problems